Chapter 19

Altering the Self-Association and Stability of Insulin by Amino Acid Replacement

David N. Brems, Patricia L. Brown, Christopher Bryant, Ronald E. Chance, Richard D. DiMarchi, L. Kenney Green, Daniel C. Howey, Harlan B. Long, Alita A. Miller, Rohn Millican, Allen H. Pekar, James E. Shields, and Bruce H. Frank

Lilly Research Laboratories, Eli Lilly and Company, Indianapolis, IN 46285

We have manipulated the amino acid sequence of insulin to speed the absorption rate from the subcutaneous injection site and to improve the storage stability. The self-association of insulin was shown to be particularly sensitive to amino acid changes in the C-terminus of the B chain. The self-association of insulin was completely abolished in some analogs, which resulted in the biological effect of faster absorption rates from the subcutaneous injection site. The storage stability of Zn-free insulin was shown to be limited by the lability of the disulfide bonds. The maintenance of the native state of insulin was shown to be important in protecting the disulfides, indicating that the storage stability of insulin is under the thermodynamic control of the conformational equilibria. The storage stability of these insulin analogs differed by 100-fold.

Altering Self-Association

Insulin association is well documented but not fully understood. The insulin association behavior is known to be complex, with the metal-free species exhibiting a pH, ionic strength, and protein concentration-dependent association pattern consisting of monomer, dimer, tetramer, and higher ordered polymers all in dynamic equilibrium *(1-6)*. The association constant for the metal-free porcine monomer-dimer equilibrium at pH 7.0 is 1.4-7.5 x 10^5 M^{-1} *(3-7)*.

The most detailed atomic information concerning insulin association comes from X-ray crystallography. A variety of crystal forms of insulin have been studied. The N- and C-termini of the B chain undergo significant conformational changes between the different crystal forms *(8-12)*. The relationship between conformational flexibility of insulin, determined from X-ray crystallography, and the self-association in solution is of considerable importance. The crystal structure of the 2-Zn hexameric form and thermodynamic studies of insulin dimerization indicate that both hydrophobic interactions and hydrogen bonding are responsible for stabilizing association *(1,2,6)*. X-ray crystallography results demonstrate that most of the non-polar dimer contacts involve the C-terminal end of the B chain, with B^{23-26} and B^{28} being the most predominant residues *(10)* (see Figure 1 for the amino acid sequence of human insulin). Association of the dimer is secured by a small antiparallel ß-sheet of hydrogen

0097–6156/93/0526–0254$06.00/0

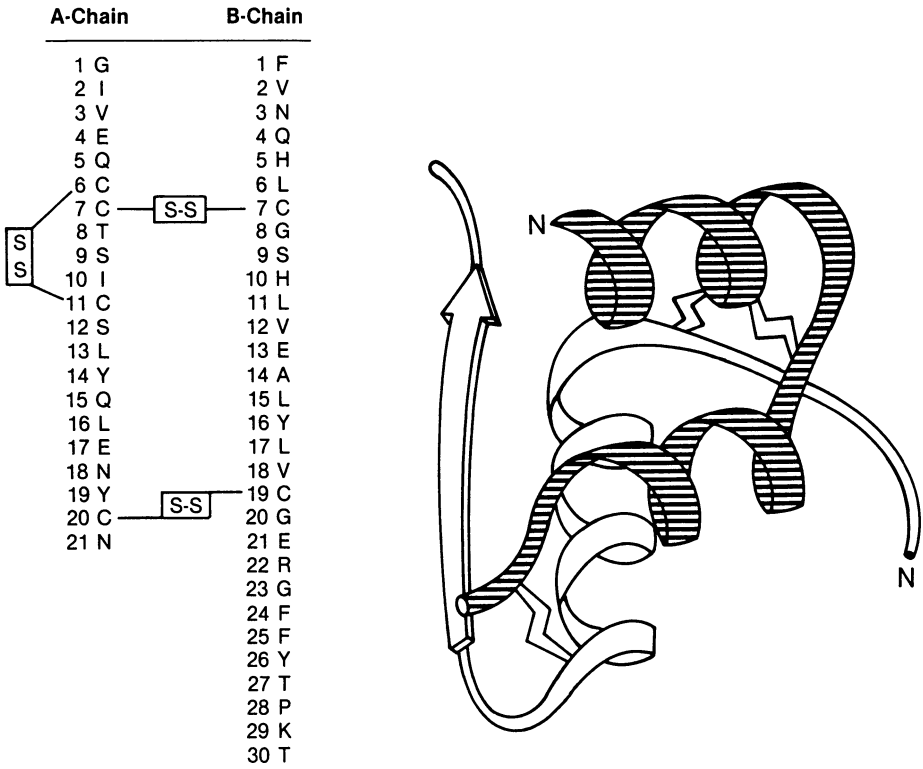

Figure 1. Amino acid sequence of human insulin and ribbon drawing of the monomeric structure (the A chain is striped).

bonds involving residues B^{24-26}. Formation of the dimer packs Pro^{B28} against residues B^{20-23}, which are in a ß-turn *(10)*. The hexamer is mainly stabilized through the Zn coordination, but additional polar and non-polar residues are buried between the dimers as a result of hexamer assembly *(10)*.

The importance of the C-terminus of the B chain is further evidenced by removal of B^{26-30} in despentapeptide insulin, which does not significantly alter the rest of the molecule but abolishes dimerization *(13)*. In this study, the C-terminus of the B chain was systematically truncated and it was established that Pro^{B28} is critical to the stabilization of insulin self-association in solution. Amino acid replacement was used to further investigate the role of B^{28} and B^{29} on self-association.

The ability to design an active insulin with diminished self-association is important for future diabetes therapy. All commercial pharmaceutical formulations contain insulin in the self-associated state and predominantly in the hexamer form *(14)*. Current models propose that the rate-limiting step in absorption of insulin from a subcutaneous injection site is the dissociation to monomer, which is readily absorbed *(15)*. Indeed, researchers at both the Novo Research Institute and the Lilly Research Laboratories have shown that monomeric insulin analogs act more rapidly than current formulations *(16, 17)*.

The Effect on Association of Truncating the C-Terminus of the B Chain. The ultracentrifugation properties of intact insulin, Des^{B30} insulin, Des^{B29-30} insulin, Des^{B28-30} insulin and Des^{B27-30} insulin, in the absence of Zn, are illustrated in Figure 2 *(see ref. 18 & 19 for experimental details)*. Removal of B^{30} or B^{29} has little effect on aggregation, but removal of B^{28-30} or B^{27-30} results in much less self-association over the concentration range of 0-5 mg/ml. The solid lines in Figure 2 represent calculated curves that best fit the experimental data. The actual data for Des^{B30} insulin and Des^{B28-30} insulin are illustrated to demonstrate the typical variation between the data and the calculated curve. We conclude from these results that B^{30} and B^{29} are not critical, but the C-terminal three amino acids are essential for stabilizing association. Removal of Pro^{B28} removes the critical intermolecular contact with B^{21}. These truncated insulins are at least 50% equipotent to insulin, as measured by receptor binding using membrane preparations of human placenta, and are at least 60% equipotent to insulin in lowering blood glucose in rats. Therefore removal of the C-terminal segment of the B chain does not destroy the conformational integrity nor activity.

The Effect on Association of Altering B^{28} and B^{29}. The ultracentrifugation properties of several insulin analogs, altered at B^{28} and/or B^{29} in the absence of Zn, are illustrated in Figure 3 *(see ref. 18 & 19 for experimental details)*. The solid lines represent the calculated curves that best fit the experimental data. The actual data for the insulin sample are illustrated to demonstrate the typical variation between the data and the calculated curve. The calculated curves in Figure 3 were obtained using an even-aggregate model of association *(5)* and the equilibrium constants were varied to achieve the best fit to the experimental data. The data are not sufficiently precise to exclude alternative models. The results show that substitution of Pro^{B28} reduces the extent of aggregation, with the least aggregation observed for $Asp^{B28} < Ala^{B28} \approx Lys^{B28}$. Variation of B^{28} plus replacement of Lys^{B29} with Pro diminishes aggregation further. For the Xaa^{B28} or the $Xaa^{B28}Pro^{B29}$ series of analogs, the least aggregation results when B^{28} is an acid side chain and the most aggregation results when B^{28} is an imino acid side chain. The equilibrium constants $K_{1,2}$ and K were determined for the analogs and are shown in Table I *(see 18 & 19 for experimental details)*. The data in Table I show that for the analogs the dimerization constants are altered more than the constant for higher order association.

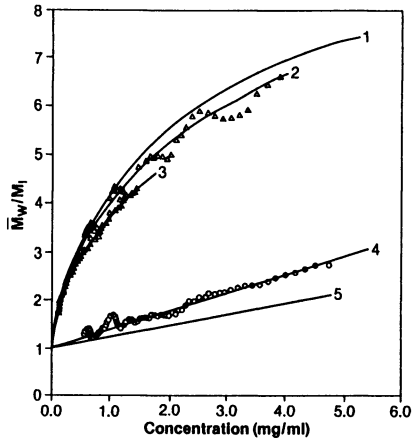

Figure 2. Equilibrium ultracentrifugation of human insulin and analogs. Effect of protein concentration of Zn-free insulin (curve 1) and Zn-free C-terminal truncated analogs: Des^{B30} insulin, curve 2; $Des^{B29\text{-}30}$ insulin, curve 3; $Des^{B28\text{-}30}$ insulin, curve 4; and $Des^{B27\text{-}30}$ insulin, curve 5. (Δ), observed data for Des^{B30} and (o), $Des^{B28\text{-}30}$ insulin. Each line represents a calculated curve that best fits the data according to the even-aggregate model of association (see Table I). M_W/M_1 represents the weight average molecular weight obtained from ultracentrifugation divided by the molecular weight of insulin monomer. (Reproduced with permission from ref. 19. Copyright 1992 IRL Press.)

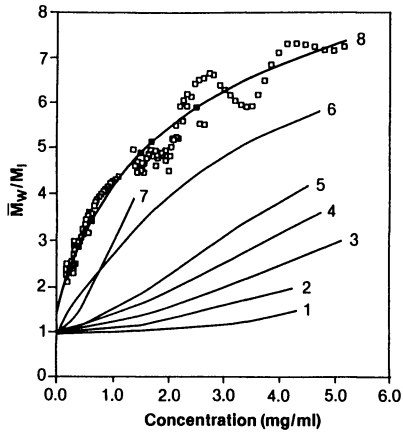

Figure 3. Equilibrium ultracentrifugation of human insulin and analogs. Effect of protein concentration on ultracentrifugation in the absence of Zn of: $Asp^{B28}Pro^{B29}$ insulin, curve 1: $Ala^{B28}Pro^{B29}$ insulin, curve 2; $Lys^{B28}Pro^{B29}$ insulin, curve 3; Pro^{B29} insulin, curve 4; Asp^{B28} insulin, curve 5; Ala^{B28} insulin, curve 6; Lys^{B28} insulin, curve 7; and insulin, curve 8. The symbols represent the observed data for insulin. Each line represents a calculated curve that best fits the data according to the even-aggregated model of association (see Table I). (Reproduced with permission from ref. 19. Copyright 1992 IRL Press.)

Table I. **Equilibrium Constants for an Even-Aggregation Model[a] as Determined by Ultracentrifugation**

Analog (Zn-free)	$K_{1,2}$ (x 10^3 M^{-1})	K_{2n+2} (x 10^3 M^{-1})
Human insulin (HI)	300	12
Ala^{B28}HI	15	7.5
Lys^{B28}HI	2.3	27
Asp^{B28}HI	1.5	6.5
Pro^{B29}HI	1.1	4.8
$Lys^{B28}Pro^{B29}$ HI	0.9	3.5
$Ala^{B28}Pro^{B29}$ HI	0.5	3.6
$Asp^{B28}Pro^{B29}$ HI	0.1	7.5

[a]Even-aggregate model $I_1 \leftrightarrow I_2 \leftrightarrow I_4 \leftrightarrow I_6 \ldots I_{12} \leftrightarrow I_{14}$. $K_{1,2} = [I_2]/[I_1]^2$ and $K_{2n+2} = [I_{2n+2}]/[I_2]\,[I_{2n}]$ where n = 1-6 *(see ref. 5 for details).*

Mechanism for Decreased Self-Association. Insulin in dilute concentrations has an altered conformation compared to insulin in more concentrated solutions *(6)*. Dilute insulin has a 15-20% increase in ß-sheet and a concomitant decrease in random coil *(20.)*. The far-UV circular dichroism data of the predominantly monomeric analogs are each similar and indistinguishable from that of dilute insulin (data not shown). Our results show that the location of a Pro residue at B^{28} is crucial for high-affinity dimerization of insulins. Thus, the absence of Pro at B^{28} in a series of C-terminal truncated insulins or amino acid replacements at B^{28} leads to decreased self-association. Replacing Lys^{B29} with Pro and varying the amino acid at B^{28} caused even greater diminution of self-association. The X-ray structure of 2-Zn insulin hexamer indicates that Pro^{B28} makes a non-bonded intermolecular contact of ≤3.5Å to B^{21}. Removal or replacement of Pro^{B28} with other amino acids destroys this critical self-association contact, and in solution disrupts dimerization to the extent shown in Table I. Lys^{B29} does not make critical intermolecular interactions as evidenced by the self-association of $Des^{B29\text{-}30}$ insulin. Charge repulsion at B^{28} is not the cause for the disruption in self-association *(21)*, because neutral, acid, and basic amino acid substitutions at B^{28} all significantly disrupt dimerization (Table I). We suggest that insertion of Pro at B^{29} creates a new surface that interferes with dimerization. The combination of removing the Pro^{B28} intermolecular contact and introducing an interfering contact with Pro at B^{29} is most effective at disrupting insulin self-association without destroying the insulin monomeric conformation.

Time-Action Profile for a Monomeric Insulin Analog. The rate-limiting step of insulin absorption from the subcutaneous injection site is thought to be the dissociation process *(15)*. Insulin analogs that are predominantly monomeric at the normal concentrations used for injection therapy (3.5 mg/ml) are expected to diffuse more quickly from subcutaneous injection to plasma circulation. $Lys^{B28}Pro^{B29}$ insulin was tested for its time-dependent activity profile in normal human volunteers. $Lys^{B28}Pro^{B29}$ insulin was chosen because it was a fully potent insulin agonist by *in vitro* binding assessment relative to insulin in IM-9 lymphocytes, glucose transport in

isolated rat adipocytes, *in vivo* activity in rats and rabbits, and that it displayed extremely weak self-association. The time action profile of $Lys^{B28}Pro^{B29}$ insulin (Zn-free) has been compared to Humulin R (Zn-human insulin formulated for commercial sale) *(17)*. The results of a randomized crossover design study in 9 healthy men using the euglycemichyperinsulinemic clamp technique *(22)* is shown in Table II.

Table II. **Human Clinical Study of the Time Action of $Lys^{B28}Pro^{B29}$ insulin compared to Humulin R**

Physiological response[a]	$Lys^{B28}Pro^{B29}$ insulin	Humulin R	pvalue[b]
Cmax[c] (ng/ml)	5.26	1.80	0.0003
Tmax[d] (hr)	0.56	2.36	0.0045
Ka[e] (1/hr)	0.829	0.373	0.0001
Rmax[f] (mg/min)	501	436	ns[g]
TRmax[h] (hr)	1.03	2.17	0.0038
DA[i] (hr)	3.60	7.10	0.0001

[a]10 units (28.57 units/mg) of each insulin injected subcutaneously (the *in vivo* potency of $Lys^{B28}Pro^{B29}$ insulin is equal to that of human insulin).

[b]analysis of variance (i.e. a value of 0.0003 implies that the differences observed in this trial are expected only 3 times in 10,000 similar trials if insulin and the analog did not really promote different time actions).

[c]peak concentration of insulin or analog.

[d]time to peak.

[e]absorption rate constant.

[f]peak glucose infusion rate.

[g]not significant.

[h]time to peak glucose infusion rate.

[i]duration of action.

Table II demonstrates that $Lys^{B28}Pro^{B29}$ insulin displays a more rapid onset and disappearance of action than Humulin R. The time action of $Lys^{B28}Pro^{B29}$ insulin more closely approximates the normal physiological response to a meal. Clinical studies are currently ongoing to assess the degree of improvement in diabetes management that might be achievable through use of this fast-acting insulin analog or other appropriate monomeric analogs.

Altering Stability

In vitro protein stability is important in all investigations regarding proteins. Lack of stability or degradation can prohibit or compromise the understanding of protein structure-function relationships. When proteins are utilized as pharmaceuticals (i.e., insulin), stability is of paramount importance to millions of patients. Formulations of insulin consist of liquid preparations that are administered by injection. Some degradation products are inactive and may cause unnecessary complications *(23)*. In current insulin formulations, every effort is made to keep insulin degradation to a minimum. The current expiration date for insulin formulations ranges from 18 to 24 months and is governed by the intrinsic degradation rate of insulin *(23-24)*. It may be

possible to increase the stability of insulin through appropriate replacement or deletions of amino acids, and thereby reduce unwanted degradation and extend the expiration time. The native state of proteins is known to provide protection against degradation, which suggests that the solution-state storage of a protein may be governed by the equilibrium constant of unfolding;

$$Keq = U / N, \quad \text{where: N = native and U = unfolded; for the reaction N <----> U.}$$

Excipients or amino acid replacements that increase the equilibrium constant are predicted to increase chemical degradation, and those that decrease the equilibrium constant are predicted to decrease chemical degradation. To establish that such a relationship exists, the rate of chemical degradation and the conformational stability of numerous insulin analogs were examined. The chemical degradation studies were conducted by incubating solutions of insulin or insulin analogs at 50°C for varying time periods and measuring the formation of large molecular weight polymers by size-exclusion chromatography. Conformational stability was determined by guanidine hydrochloride (GdnHCl)-induced equilibrium denaturation *(25)*.

Chemical Stability. Insulin and analogs were stored at 50°C for varying times. Chemical degradation accelerates at a temperature of 50°C but heat denaturation is not induced (unpublished results). Degradation at 50°C was detected by size-exclusion chromatography and the results are illustrated in Figure 4 *(see ref. 18 & 19 for experimental details)*. The chromatography mobile phase contained 6M GdnHCl to disrupt any noncovalent self-association of insulin. Therefore, peaks eluting earlier than monomer represent covalent adducts of insulin. The primary degradation product is a large molecular weight polymer that elutes near the exclusion limit of the column. When DTT was added to a sample that had been degraded for 6 days, the polymer disappeared (Figure 4) and reduced to authentic insulin A chain and insulin B chain, as determined by RP-HPLC (data not shown). Peaks eluting after 720 s (Figure 4) correspond to the buffers and preservatives that were present in the incubation mixture.

The mechanism of the large molecular weight polymer formation was explored. Table III *(see ref. 18 & 19 for experimental details)* shows that the rate of polymer formation is dependent on pH, temperature, and metal ions.

Table III. **Effect of pH, Metal Ion, and Temperature on the Rate of Polymer Formation** [a,b]

	50°C				40°C	30°C
	pH 9	pH 8	pH 7.4	Cu^{2+}(pH 8)[c]	pH 8	pH 8
Human insulin[d]	12.4	15	139	56	392	4029

[a]Polymer was detected by size-exclusion chromatography using 6M GdnHCl, 0.1M phosphate, pH 3.0, as the eluting solvent.

[b]Values are half-lives, in days, determined from the slope of a plot of the ln of the area of the high molecular weight polymer peak versus time.

[c]100 μM Cu^{2+}.

[d]3.5 mg/ml.

The polymerization rate increases with increasing pH, suggesting that the mechanism is dependent on the concentration of hydroxyl ions. The polymerization rate increases with higher temperatures. Redox metal ions, such as Cu^{2+}, retard the polymerization

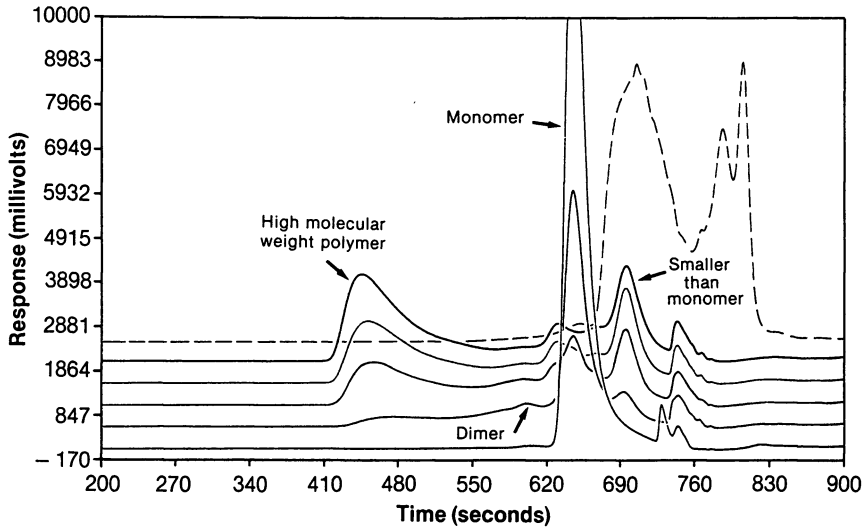

Figure 4. Size-exclusion chromatography of human insulin incubated for varying time periods at 50°C, in 0.1 M sodium phosphate, pH 8.0, 0.25% m-cresol and 1.6% glycerol. The bottom chromatogram sample was not incubated, and in ascending order the chromatograms were incubated for 1, 2, 3, and 6 days, and 6 days with DTT added after incubation but prior to chromatography (dashed line). The chromatography elution solvent was 6M GdnHCl, 0.1M sodium phosphate, pH 3.0. (Reproduced with permission from ref. 18. Copyright 1992 IRL Press.)

reaction (the oxidized form is required for the retardation). These results are consistent with a β-elimination mechanism of the disulfide bonds and a disulfide interchange reaction, as previously established by Zale and Klibanov (26) as a major degradation pathway for insulin at 100°C. The polymerization rate of metal-free insulin at 40 and 30°C was explored and the results are shown in Table III. At all temperatures tested, a high molecular weight polymer is the major degradation product. The rate of polymerization was linear with respect to temperature over the range investigated. For insulin, 50°C is an accelerator for chemical degradation and is representative of the polymerization mechanism that occurs at lower temperatures. The possibility that the OH^- concentration and metal ions affect the rate of polymerization by altering the equilibrium constant for self-association has been considered. However, monomeric analogs that remain monomeric under the variations of Table III still behave as expected for a ß-elimination and disulfide interchange mechanism. The rate of polymerization to high molecular weight forms at 50°C was investigated for numerous insulin analogs. The results for the rate of polymerization for analogs and insulin are illustrated in Figures 5 and 7 *(see ref. 18 & 19 for experimental details)*. As can be seen in Figure 5, the polymerization rate of insulin analogs varies greatly, with $Asp^{B10}Asp^{B28}Pro^{B29}$ insulin demonstrating greater stability and $Lys^{B28}Pro^{B29}$ insulin showing lesser stability compared with insulin.

Conformational Stability. Guanidine hydrochloride-induced equilibrium denaturation was utilized to determine the conformational stability of insulin and insulin analogs. Denaturation was measured by circular dichroism at 224 nm. Previous studies of insulin have established that the denaturation transitions are reversible and conform to a two-state mechanism, with the two states being monomeric native and monomeric denatured *(27)*. The denaturation experiments contained 20% ethanol to disrupt insulin self-association and to avoid the complications of intermolecular interactions *(27)*. Figures 6, 7, and Table IV *(see ref. 18 & 19 for experimental details)* show the equilibrium denaturation results for numerous insulin analogs. Figure 6 shows the equilibrium denaturation results for insulin, $Lys^{B28}Pro^{B29}$ insulin (the least stable analog), and $Asp^{B10}Asp^{B28}Pro^{B29}$ insulin (the most stable analog). The free energy of unfolding varies by 2 kcal/mol (Figure 6 & Table IV) for the different analogs. The majority of analogs belong to a related series for which Lys^{B29} was changed to proline and B^{28} was varied. In this series of analogs, the conformational stabilities are comparable or less than that for insulin. Changing His^{B10} to aspartic acid significantly increased the free energy of unfolding. The effect of Asp^{B10} was also evident for analogs in which the C-terminus was altered. We suggest that the stabilizing effect of Asp^{B10} and the $Xaa^{B28}Pro^{B29}$ could be caused by a positive helix dipole effect *(28-30)* or a hydrogen bond acceptor near the N-terminal end of a helix *(31-32)*. Residues B^{9-19} form an α-helix containing a net helix dipole of one positive charge near B^9 and one negative charge near B^{19} (Figure 1). A negative charge at B^{10} from an aspartic side chain might be expected to favorably interact with the positive charge dipole and cause a net stabilization of the helix and an overall increase in the protein's conformational stability. An alternative explanation for the stabilizing effect of Asp^{B10} is that the ß-carboxyl of aspartic acid can form hydrogen bonds with any of the initial four main chain NH groups of the helix B^{9-19} that are otherwise unpaired.

Correlation of Chemical and Conformational Stability. Figure 7 shows the rate of chemical degradation versus the midpoint of denaturation for the different insulin analogs. The straight line in Figure 7 was determined by a least-squares fit to the data and has an R^2 value of 0.7 and $P < 0.0005$. Insulin analogs with the greatest chemical stability have the largest midpoint of denaturation and those analogs with the least chemical stability have the smallest midpoint of denaturation. The positive correlation for the rate of polymerization versus the midpoint of denaturation indicates that the

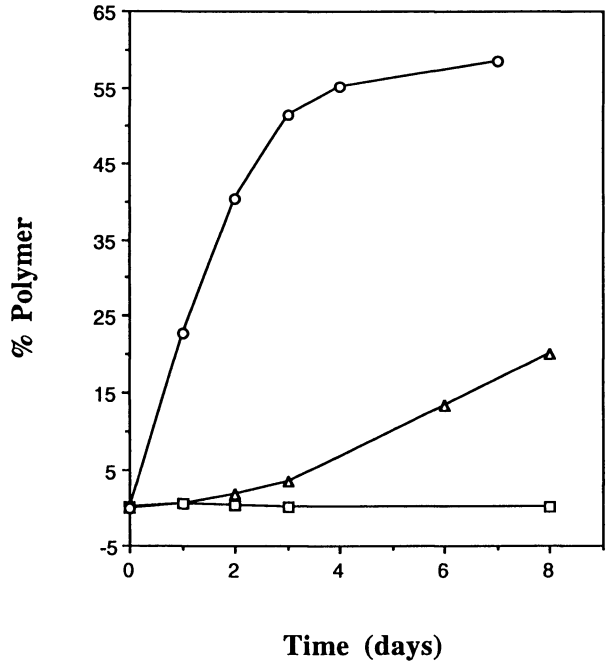

Figure 5. Stability to chemical degradation (tendency to form polymers). Human insulin (Δ), $Asp^{B10}Asp^{B28}Pro^{B29}$ insulin (□), and $Lys^{B28}Pro^{B29}$ insulin (○) were incubated for various times at 50°C as in Figure 4 except at pH 7.4. The formation of polymer was determined by size-exclusion chromatography with 6M GdnHCl, 0.1M sodium phosphate, pH 3 as the chromatography elution solvent. (Reproduced with permission from ref. 18. Copyright 1992 IRL Press.)

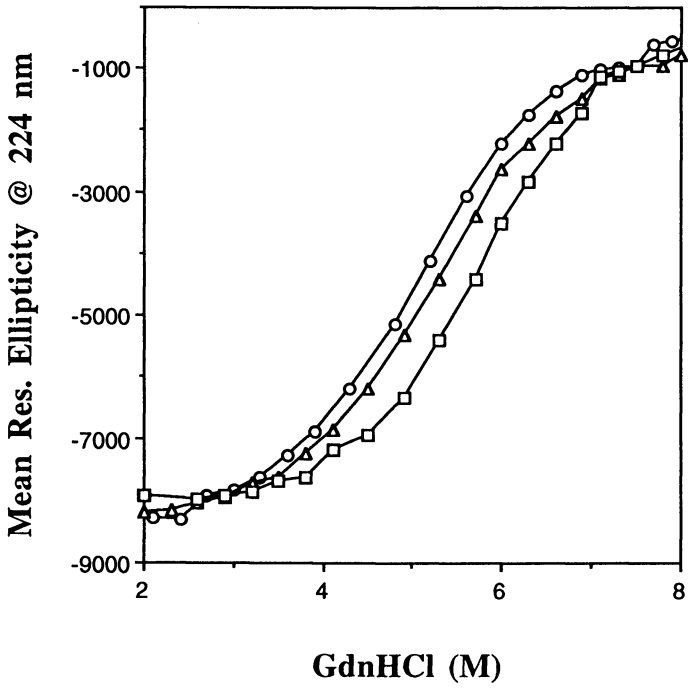

Figure 6. Stability of the conformational equilibria. GdnHCl-induced equilibrium denaturation of insulin (Δ), $Asp^{B10}Asp^{B28}Pro^{B29}$ insulin (□), and $Lys^{B28}Pro^{B29}$ insulin (o), measured by far-UV CD as described in ref. 27. (Reproduced with permission from ref. 18. Copyright 1992 IRL press.)

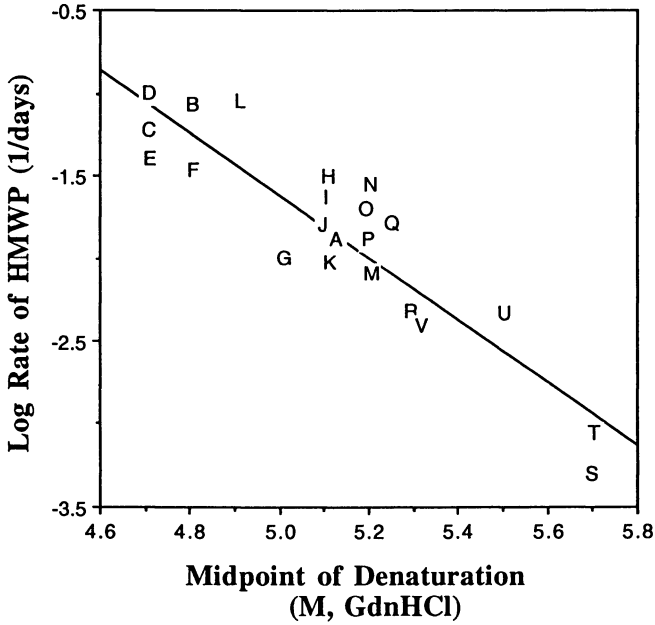

Figure 7. Correlation between chemical stability and conformational stability. Chemical stability was determined by the tendency to form polymer at 50°C as in Figure 4. Conformational stability was estimated by the transition midpoint of the GdnHCl-induced equilibrium denaturation as described in ref. 27. The letter code for each analog is contained in Table IV. (Reproduced with permission from ref. 18. Copyright 1992 IRL press.)

chemical stability of insulin is under the thermodynamic control of the protein conformational equilibria.

Since the main pathway for chemical degradation for Zn-free insulin is through disulfide destruction, we explored the rate of chemically induced reduction of protein disulfides for the analogs that differed the most in chemical and conformational stability. Insulin or insulin analogs were exposed to DTT for varying times and disulfide reduction was determined by reversed-phase chromatography. The results of such an experiment are illustrated in Figure 8 *(see ref. 18 & 19 for experimental details)*. The ordinate in Figure 8 represents the percent insulin that remains native or unreacted. As can be seen in Figure 8, $Asp^{B10}Asp^{B28}Pro^{B29}$ insulin is the most resistant to reduction, insulin showed intermediate susceptiblity, and $Lys^{B28}Pro^{B29}$ insulin was the most labile. To verify that the different susceptibilities observed for insulin and its analogs are conformationally related, the reduction was carried out in denaturing concentrations of GdnHCl. The results of this control experiment are illustrated in Figure 8 and demonstrate that the susceptibility to reduction of insulin and its analogs is indistinguishable in GdnHCl. Guanidine hydrochloride was shown not to alter the reducing potential of the reaction mixture by measuring the rate of DTT-induced reduction of glutathione in the presence and absence of GdnHCl (data not shown). Therefore, different susceptibilities observed for insulin in the presence and absence of denaturant is a measure of the disulfide protection provided by the native structure. In order to develop $lys^{B28}pro^{B29}$ insulin as a commercial product of

Table IV. **Results from Equilibrium Denaturation**

Code	Insulin analog	Midpoint[a] (M GdnHCl)	ΔG (kcal/mol)[b]
A	human insulin (HI)	5.1	4.4
B	A^{B28}-HI	4.8	4.0
C	des^{B23-30}-HI	4.7	3.8
D	$W^{B28pB29}$-HI	4.7	3.9
E	$L^{B28pB29}$-HI	4.7	4.2
F	$S^{B28pB29}$-HI	4.8	4.0
G	des^{B30}-HI	5.0	4.6
H	$F^{B28pB29}$-HI	5.1	4.9
I	G^{B29}-HI	5.1	4.3
J	$G^{B28pB29}$-HI	5.1	4.6
K	$Q^{B28pB29}$-HI	5.1	4.8
L	$K^{B28pB29}$-HI	4.9	3.6
M	$E^{B28pB29}$-HI	5.2	4.6
N	$A^{B28pB29}$-HI	5.2	4.8
O	$Aba^{B28pB29}$-HI	5.2	5.4
P	$V^{B28pB29}$-HI	5.2	4.7
Q	$D^{B10}K^{B28pB29}$-HI	5.3	4.7
R	D^{B10}-HI	5.3	5.1
S	$D^{B10}V^{B28pB29}$-HI	5.7	4.9
T	$D^{B10}D^{B28pB29}$-HI	5.7	5.7
U	$D^{B10}E^{B28pB29}$-HI	5.5	5.2
V	$D^{B10}Q^{B28pB29}$-HI	5.3	5.4

[a]The midpoint of the denaturation transition where: Keq = U/N = 1. Repetitive measurements of separate sample preparations show a variation of ±0.1 M GdnHCl.

[b]Gibbs free energy of unfolding in the absence of denaturant, which equals ΔG + m (GdnHCl), where m is a measure of the dependence of ΔG on [GdnHCl]. Repetitive measurements of separate sample preparations show a variation of ±0.5 kcal/mol.

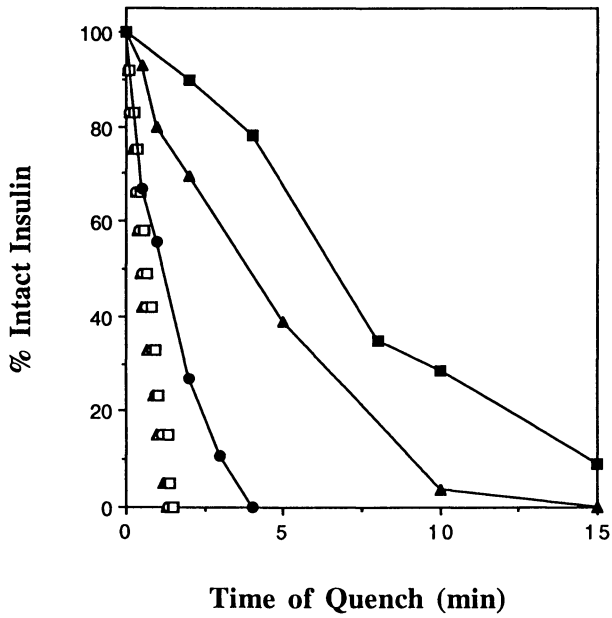

Figure 8. Susceptibility to reduction. Insulin (▲), $Lys^{B28}Pro^{B29}$ insulin (●), and $Asp^{B10}Asp^{B28}Pro^{B29}$ insulin (■) at a concentration of 1.2 mg/ml were incubated in a reducing solution containing 25 mM DTT, pH 7.5, 0.2 M Tris at 23°C, and at various times samples were withdrawn, quenched in acid and analyzed for unreduced (intact) insulin by reversed-phase HPLC *(18)*. The open symbols are the results when the reducing solution contained 7 M GdnHCl. (Reproduced with permission from ref. 18. Copyright 1992 IRL Press.)

adequate stability, an alternative strategy that incorporates stabilizing additives into the formulation will need to be developed. Instability is not inherent to monomeric insulins as demonstrated by the extreme stability of analogs containing asp^{B10}.

We conclude the different rates of polymer formation for the analogs are caused by the differing extents of susceptibility of their disulfide bonds which, in turn, are dependent on the equilibrium constant of unfolding for the conformational equilibria of the insulin analog. These results confirm that the chemical stability of insulin is under the thermodynamic control of the conformational equilibrium constant for unfolding, which indicates that the rate of polymer formation is greater from the unfolded than the folded state.

Literature Cited

1) Fredericq, E. *Arch. Biochem. Biophys.,* **1956**, *65*, 218-228.
2) Jeffrey, P. D.; Coates, J. H. *Biochemistry*, **1966**, *5*, 489-498.
3) Pekar, A. H.; Frank, B. H. *Biochemistry*, **1972**, *11*, 4013-4016.
4) Goldman, J.; Carpenter, F. H. *Biochemistry*, **1974**, *13*, 4566-4574.
5) Jeffrey, P. D.; Milthorpe, B. K.; Nichol, L. W. *Biochemistry,* **1976**, *15*, 4660-4665.
6) Pocker, Y.; Biswas, S. B. *Biochemistry,* **1981**, *20*, 4354-4361.
7) Strazza, S.; Hunter, R.; Walker, E.; Darnall, D. W. *Arch. Biochem. Biophys.*, **1985**, *238*, 30-42.
8) Bentley, G.; Dodson, E.; Dodson, G.; Hodgkin, D.; Mercola, D. *Nature*, **1976**, *261*, 166-168.
9) Chothia, C.; Lesk, A. M.; Dodson, G. G.; Hodgkin, D.C. *Nature*, **1983**, *302*, 500-505.
10) Baker, E. N.; Blundell, T. L.; Cutfield, J. F.; Cutfield, S. M.; Dodson, E. J.; Dodson, G. G.; Crowfoot Hodgkin, D. M.; Hubbard, R. E.; Isaacs, N. W.; Reynolds, C. D.; Sakabe, K.; Sakabe, N.; Vijayan, N. M. *Phil. Trans. R. Soc. Lond., B,* **1988**, *319*, 369-456.
11) Derewenda, U.; Derewenda, Z.; Dodson, E. J.; Dodson, G. G.; Reynolds, C. D.; Smith, G. D.; Sparks, C.; Swenson, D. *Nature*, **1989**, *338*, 594-596.
12) Badger, J.; Harris, M. R.; Reynolds, C. D.; Evans, A. C.; Dodson, E. J.; Dodson, G. G.; North, A. C. T. *Acta Crystallogr.,* **1991**, *B47*, 127-136.
13) Bi, R. C.; Dauter, Z.; Dodson, E. J.; Dodson, G. G.; Giordano, F.; Reynolds, C. D. *Biopolymers,* **1984**, *32*, 391-395.
14) Blundell, T. L.; Dodson, G. G.; Hodgkin, D. C.; Mercola, D. *Adv. Protein Chem.*, **1972**, *26*, 279-402.
15) Binder, C. In *Artificial Systems for Insulin Delivery;* Brunetti, P.; Alberti, K. G. M. M.; Albisser, A. M.; Hepp, K. D.; MassiBendetti, M., Eds.; Raven Press: New York, 1983; pp. 53-57.
16) Brange, J.; Dodson, G. G.; Xiao, B. *Curr. Opin. Struct. Biol.*, **1991**, *1*, 934-940. *8*, 280-286.
17) DiMarchi, R.D.; Mayer, J.P.; Fan, L.; Brems, D.N.; Frank, B.H.; Green, L.K.;, Hoffmann, J.A.; Howey, D.C.; Long, H.B.; Shaw, W.N.; Shields, J.E.; Slieker, L.J.; Su, K.S.E.; Sundell, K.L.; Chance, R.E. In *Peptides: Chemistry and Biology, Proceedings of the Twelfth American Peptide Symposium;* Smith, J.E.; Rivier, J.E., Eds; ESCOM, Leiden, 1992; pp. 26-28.
18) Brems, D. N.; Brown, P. L.; Bryant, C.; Chance, R. E.; Green, L. K.; Long, H. B.; Miller, A. A.; Millican, R.; Shields, J. E.; Frank, B. H. *Protein Engineering*, **1992**, *5*, 519-525.
19) Brems, D. N.; Alter, L. A.; Beckage, M. J.; Chance, R. E.; DiMarchi, R. D.; Green, L. K.; Long, H. B.; Pekar, A. H.; Shields, J. E.; Frank B. H. *Protein Engineering*, **1992**, *5*, 527-533.

20) Melberg, S. G.; Johnson, W. C., Jr. *Proteins: Struct. Funct. Genet.*, **1990**,
21) Brange, J.; Ribel, U.; Hansen, J. F.; Dodson, G.; Hansen, M. T.; Havelund, S.; Melberg, S. G.; Norris, F.; Norris, K.; Snel, I.; Sorensen, A. R.; Voigt, H. O. *Nature*, **1988**, *333*, 679-682.
22) Andres, R.; Swerdloff, R.; Pozefsky, T.; Coleman, D. In *Automation in Analytical Chemistry;* Skeggs, L.T. Jr., Ed.; Medaid: New York, NY, 1966; pp. 486-491.
23) Brange, J. *Galenics of Insulin;* Springer Verlag: New York, NY, 1987; pp. 1-101.
24) In *United States Pharmacopeia*; XXII Mack Printing Co.: Easton, Rockville, PA, 1990; pp. 692-700, 1513-1514..
25) Pace, C. N. *Methods Enzym.*, **1986**, *131*, 266-280.
26) Zale, S. E.; Klibanov, A. M. *Biochemistry,* **1986**, *25*, 5432-5444.
27) Brems, D. N.; Brown, P. L.; Heckenlaible, L. A.; Frank, B. H. *Biochemistry*, **1990**, *29*, 9289-9293.
28) Hol, W. G. J. *Prog. Biophys. Molec. Biol.*, **1985**, *45*, 149-195.
29) Shoemaker, K. R.; Kim, P. S.; York, E.; Stewart, J. M.; Baldwin, R. L. *Nature*, **1987**, *326*, 563-567.
30) Fairman, R.; Shoemaker, K. R.; York, E. J.; Stewart, J. M.; Baldwin, R. L. *Proteins: Struct., Funct., Genet.*, **1989**, *5*, 1-7.
31) Presta, L. G.; Rose, G. D. *Science,* **1988**, *240*, 1632-1641.
32) Richardson, J. S.; Richardson, D. C. *Science*, **1988**, *240*, 1648-1652.

RECEIVED November 11, 1992